ARCHIVES OF ELECTRICAL ENGINEERING VOL. 67(4), pp. 939–953 (2018)

DOI 10.24425/aee.2018.124834

Analysis of the influence of inverter PWM speed control methods on the operation of a BLDC motor

MAREK PAWEL CIURYS

Department of Electrical Machines, Drives and Measurements
Faculty of Electrical Engineering, Wrocław University of Science and Technology
e-mail: marek.ciurys@pwr.edu.pl

(Received: 06.06.2018, revised: 26.09.2018)

Abstract: An analysis of the influence of inverter PWM speed control methods on the operation of a brushless DC (BLDC) motor was carried out. Field-circuit models of the BLDC motor were developed taking into account rotational speed control by two classic methods: the unipolar H_ON_L_PWM and the bipolar H_PWM_L_PWM. Waveforms of the electrical and mechanical quantities and the motor parameters were computed. The results of the computations were verified by measurements performed on a specially designed test stand. On the basis of the measured waveforms of the electrical and mechanical quantities the dependence of the drive system efficiencies and power losses on rotational speed was determined for the two methods of inverter control.

Key words: analysis, brushless DC motors, electrical machines, PWM speed control, measurements

1. Introduction

In brushless DC motors, on the basis of the rotor position data, the control system generates impulses controlling the operation of the electronic commutator supplying the stator winding phases. The phases are supplied in such a way as to ensure perpendicularity between the stator and rotor fields. Each transistor of the electronic commutator (Fig. 1) conducts current for a period of 120 electric degrees, while the phases are switched every (Fig. 2) 60 degrees [1, 2].

Since the rotational speed of BLDC motors is proportional to the power supply voltage it can be regulated using an inverter by changing the pulse width modulation duty cycle [2, 3, 4]. The PWM methods, most commonly used for this purpose, are shown in Figs. 3–7. If both, the upper (T1, T3, T5) and lower (T2, T4, T6) inverter transistors (Fig. 3) are used to control the speed, the method is referred to as bipolar (H_PWM_L_PWM) [3, 4]. When only the upper transistors or the lower transistors are used, the method is referred to as unipolar H_PWM_L_ON (Fig. 4) or H_ON_L_PWM (Fig. 5), respectively.

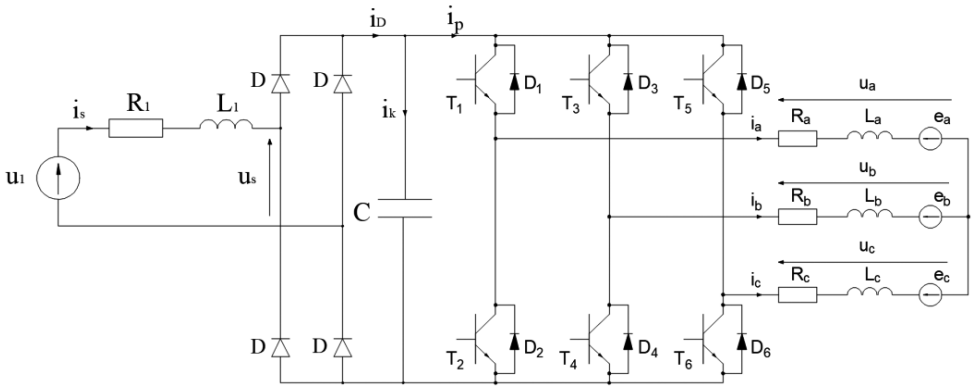

Fig. 1. Diagram of the single phase AC network-converter (rectifier-capacitor-inverter)-brushless DC motor system

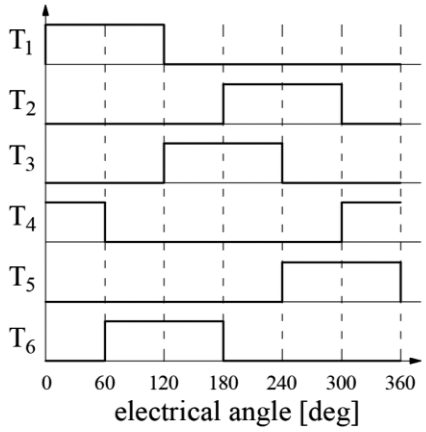

Fig. 2. Commutation sequence of the transistors without PWM inverter operation

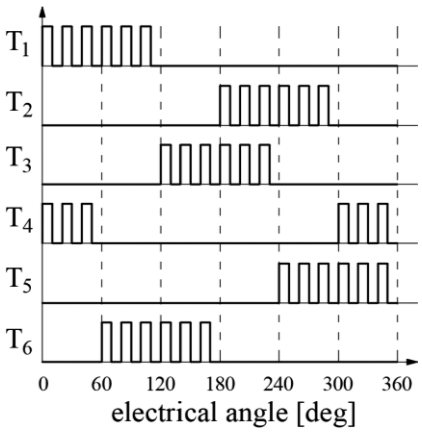

Fig. 3. Switching sequence of the inverter transistors for the H_PWM_L_PWM method

For the unipolar ON_PWM method the inverter transistors perform the regulatory function only during the last 60 electrical degrees of their conduction period, i.e. they are switched at the PWM frequency (Fig. 6). In the case of the PWM_ON method, all the transistors perform the regulatory function for the first 60 electrical degrees of their conduction period (Fig. 7).

PWM inverter operation with a frequency from a few to a few tens of kHz causes phase current pulsations. Due to the changes in magnetic flux density caused by the stator slotting and the phase current pulsations resulting from commutation and inverter PWM operation, power losses occur in the permanent magnets and in the rotor core [5–9].

The changes in current values cause a change in the distribution and pulsations of magnetic flux density, also in the stator. This has a bearing on power losses in the motor stator [10–12] and results in a change in winding inductance, thereby affecting the instantaneous values of the

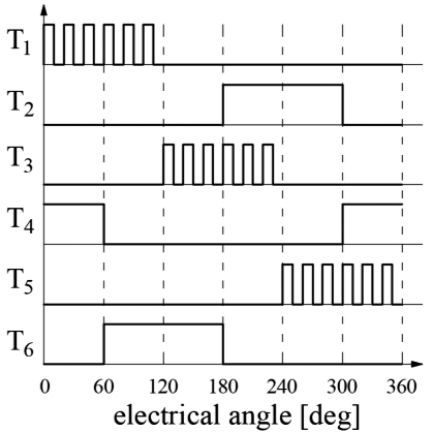

Fig. 4. Switching sequence of the inverter transistors for the H_PWM_L_ON method

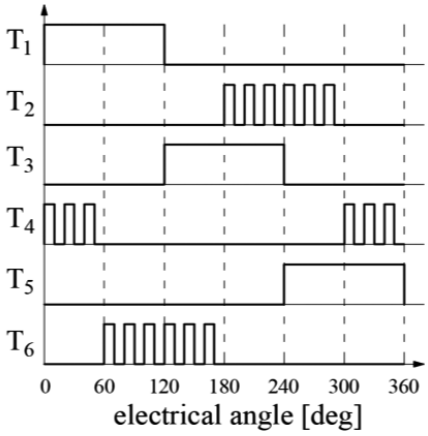

Fig. 5. Switching sequence of the inverter transistors for the H_ON_L_PWM method

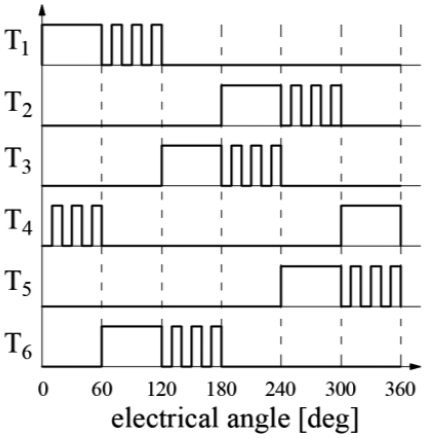

Fig. 6. Switching sequence of the inverter transistors for the ON_PWM method

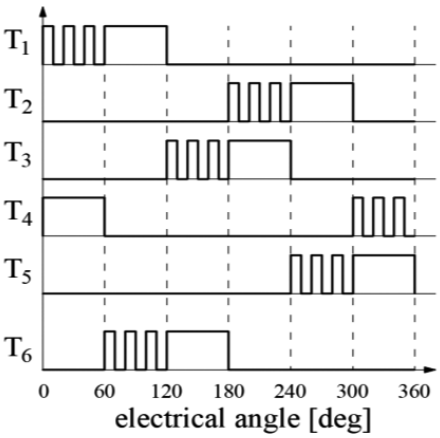

Fig. 7. Switching sequence of the inverter transistors for the PWM_ON method

electrical quantities in the drive system. The waveforms of electrical and mechanical quantities, the operating parameters and the electromagnetic phenomena in the BLDC motor drive system depend on the PWM method used for speed control.

To the author's knowledge, the issues concerning the influence of the inverter PWM control methods on the waveforms and operation of BLDC motors have not been sufficiently discussed. The issues found in the literature usually concern selected physical quantities, e.g. torque pulsations or phase current waveforms. Moreover, such analyses are usually performed using circuit models which do not take into account saturation in the magnetic circuit and changes in motor winding inductance.

The aim of this paper is to compare the influence of bipolar (H_PWM_L_PWM) and unipolar H_ON_L_PWM control methods on the waveforms of the electrical and mechanical quantities of the BLDC motor and its operation. Further in this paper the methods will be referred to as the bipolar method and the unipolar method, respectively.

The scope of this research work included:

– the design and construction of a BLDC motor and a power converter,
– the development of field-circuit models, taking into account the unipolar method and the bipolar method,
– the computation of the waveforms of electrical and mechanical quantities and the determination of drive system losses and efficiencies for the two considered control methods,
– the design and construction of a test stand,
– the measurement of the waveforms of the electrical and mechanical quantities in the drive system for the two methods of inverter PWM speed control,
– the determination of the dependence of the drive system losses and efficiencies on rotational speed for the two control methods,
– an analysis of the results.

The analysis concerns stationary states. An analysis of the operation of the drive system in dynamic states will be the subject of a separate paper.

2. Motor specifications

A computational analysis and tests of a brushless motor intended for driving an inverted action high-pressure vane pump built into the motor rotor (Fig. 8) were carried out. The design of the developed solution is discussed in detail in [13–15]. The BLDC motor is excited by neodymium magnets type REN33UH. Its power is $P = 2.5$ kW at the maximum speed of $n_{\max} = 3\,000$ rpm. The speed control range is 500–3 000 rpm. The motor is supplied from a single-phase 230 VAC, 50 Hz network through a specially designed and built converter (Fig. 1) consisting of a rectifier, a smoothing capacitor and an inverter.

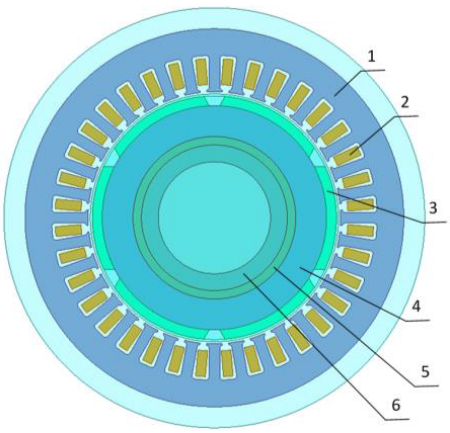

Fig. 8. Cross section of the designed motor with the built-in vane pump: 1 – stator sheet; 2 – winding; 3 – permanent magnet; 4 – rotor yoke; 5 – non-magnetic sleeve; 6 – rotating part of the vane pump

3. Field-circuit models

Field-circuit models of the analysed single phase AC network–rectifier–inverter–BLDC motor system (Fig. 1) were developed for the two considered control methods, using ANSYS Maxwell software. The models take into account, inter alia [13]:

- the geometric dimensions of the magnetic circuit of the machine,
- the parallel direction of magnets magnetization,
- the magnetization characteristics and conductivity of the stator sheet and the rotor yoke,
- the demagnetization characteristics and conductivity of the permanent magnets,
- power losses due to eddy currents and to hysteresis in the stator and in the rotor,
- the source voltage waveform (u_1) and the power supply network parameters (R_1, L_1),
- the parameters of the converter (the rectifier, the smoothing capacitor and the inverter),
- the motor winding resistance and inductance,
- the fact that the instantaneous values of motor phase currents are limited to the level which does not cause demagnetization of the magnets.

The field-circuit model of the analysed system is described in details in [13].

Due to the limited length of this paper only the main equations of the BLDC motor mathematical model of the analysed single phase AC network–rectifier–inverter–BLDC motor system are presented.

The instantaneous values of the voltages of phases "a", "b" and "c" are as follows:

$$\begin{aligned} u_a &= R \cdot i_a + (L + L_p - M) \cdot \frac{\mathrm{d}\, i_a}{\mathrm{d}\, t} + e_a \,, \\ u_b &= R \cdot i_b + (L + L_p - M) \cdot \frac{\mathrm{d}\, i_b}{\mathrm{d}\, t} + e_b \,, \\ u_c &= R \cdot i_c + (L + L_p - M) \cdot \frac{\mathrm{d}\, i_c}{\mathrm{d}\, t} + e_c \,, \end{aligned} \tag{1}$$

where: i_a, i_b, i_c are the instantaneous values of the currents in winding phases "a", "b" and "c"; R is the winding resistance; L is the self-inductance of the armature winding; L_p is the leakage inductance of the end winding; M is the mutual inductance of the armature winding; e_a, e_b, e_c are the instantaneous values of the back emfs induced in the winding phases.

The equation of the currents at the motor star node is

$$i_a + i_b + i_c = 0. \tag{2}$$

The instantaneous value of the motor electromagnetic torque equals

$$T_e = \frac{e_a \cdot i_a + e_b \cdot i_b + e_c \cdot i_c}{\omega} \,. \tag{3}$$

The rotor angular speed ω is

$$\omega = \frac{\mathrm{d}\, \alpha}{\mathrm{d}\, t} \,, \tag{4}$$

where: α is the rotor position angle.

The equation of motion has the form:

$$T_e(t) - T_f(t) - \Delta T(t) - T_o(t) = J\frac{\mathrm{d}\,\omega}{\mathrm{d}\,t}, \tag{5}$$

where: $T_f(t)$ is the friction torque; $\Delta T(t)$ is the torque loss (including eddy current power losses) in the rotor of the motor; $T_o(t)$ is the load torque; J is the moment of inertia of the motor with the rotating part of the vane pump.

The instantaneous value of the motor mechanical torque is

$$T(t) = T_e(t) - T_f(t) - \Delta T(t). \tag{6}$$

4. Computational analysis of the drive system

Using the field-circuit models, the waveforms of the electrical and mechanical quantities in the drive system were computed for the two control methods. The inverter PWM frequency was 15 625 Hz in both cases and the time step was set to 2 μs (32 samples per one period of operation of the PWM system). The time step corresponded to the signal sampling period used in the motor laboratory tests. The waveforms of the electrical and mechanical quantities in the drive system were determined under the load of the rated motor torque (8 Nm) at the speed of 1 500 rpm (typical of the vane pump for which the motor was designed). In order to achieve this rotational speed, the pulse width modulation duty cycle was set to 0.325 for the unipolar method and to 0.64 for the bipolar method.

The computed waveforms of the electrical and mechanical quantities (Figs. 9–18) in the single-phase AC network-converter (rectifier-capacitor-inverter)-BLDC motor system are deformed. The deformations result from voltage pulsations at the inverter input, the commutation of winding phases, the inverter PWM operation, and magnetic flux density pulsations in the magnetic circuit due to the stator slotting and phase current pulsations.

The converter input voltage waveform (Figs. 9, 10) is a distorted sine wave. This is a result of source voltage deformation and voltage drops in the single-phase AC network due to the

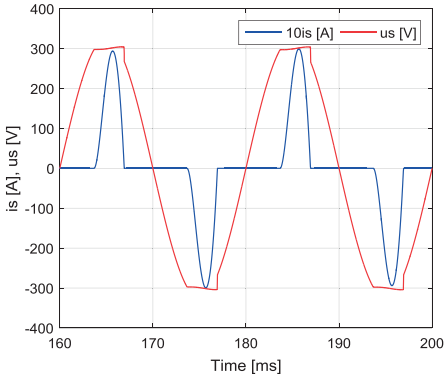

Fig. 9. Converter input current (*is*) and converter input voltage (*us*) as a function of time for the bipolar method

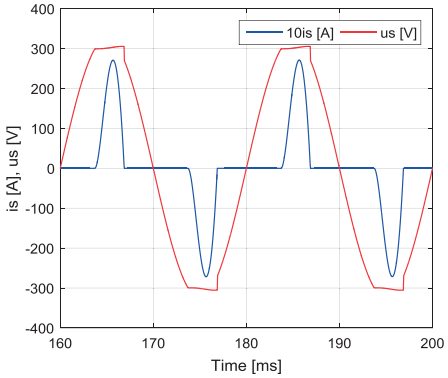

Fig. 10. Converter input current (*is*) and converter input voltage (*us*) as a function of time for the unipolar method

discontinuous current drawn by the converter. The peak value of this current reaches 30.1 A for the bipolar method and 27.0 A for the unipolar method.

The inverter input voltage is a pulsating voltage (100 Hz) corresponding to the double network frequency. This results from the operation of the rectifying bridge–smoothing capacitor system. The voltage pulsations at the inverter input are transferred to the waveforms of the phase voltages. As a result, the amplitude of the phase currents changes over time. Because of the low inductance of the winding phases, i.e. the low value of the electromagnetic time constant, also the 15 625 Hz pulsations due to inverter PWM operation occur in the phase current waveforms (Figs. 11, 12). The switching frequency of the motor winding phases is proportional to the rotational speed. During one motor rotation, the motor winding phases are switched 18 times, i.e. the switching frequency is 450 Hz at speed $n = 1\ 500$ rpm (at $p = 3$, where p is the number of motor pole pairs).

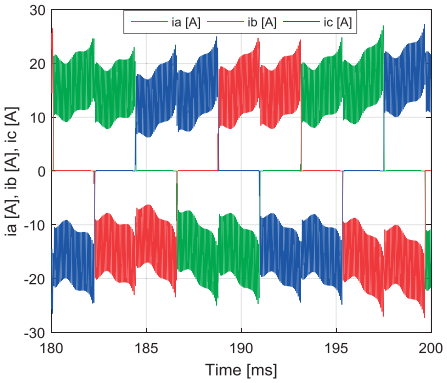

Fig. 11. Motor phase currents as a function of time for the bipolar method

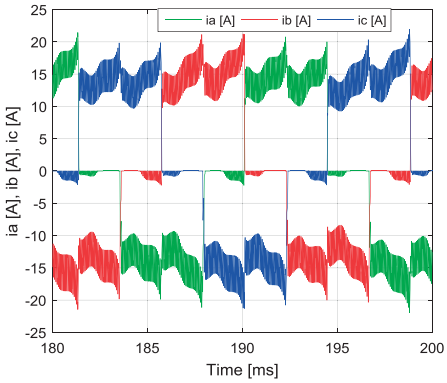

Fig. 12. Motor phase currents as a function of time for the unipolar method

For both the bipolar method and the unipolar method, the pulsations caused by inverter PWM operation and the ones caused by motor winding phase commutation predominate in the phase current waveforms (Figs. 11, 12). The pulsations of 100 Hz resulting from the operation of the rectifier system are much smaller. The pulsations of phase currents in the BLDC motor are discussed in detail in [16].

The maximum value of phase currents reaches 27.4 A for the bipolar method and 22.2 A for the unipolar method. Phase current pulsations with the PWM frequency amount to about 10 A for the bipolar method, whereas for the unipolar method they are smaller (amounting to about 5 A). Such a significant difference in the pulsation amplitude of the phase currents for both the methods is due to the fact that in the case of the bipolar method when the transistors belonging to the inverter's upper group and its lower group are switched off simultaneously, the voltage supplied to the motor winding phases is changed to the opposite polarity. This results in a faster discharge of their magnetic energy, i.e. a faster decrease in the value of the phase currents. In the case of the unipolar method, when the "control" transistor is switched off, the motor winding phases are connected via one of the transistors and one of the diodes in the upper inverter group. The steepness in current decrease in this circuit results from the electromotive forces induced in the motor phases, the motor winding parameters and the parameters of the inverter power electronics components.

The pulsations of motor phase currents cause torque pulsations. Because of the higher values of phase current pulsations in the case of the bipolar method, also torque pulsations are higher (Figs. 13, 14), amounting to 116% of the mean value, while for the unipolar method they amount to 85% of the mean value.

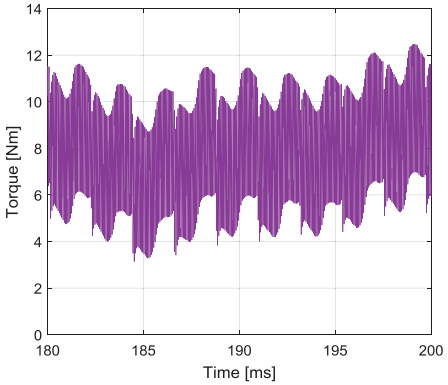

Fig. 13. Motor torque as a function of time for the bipolar method

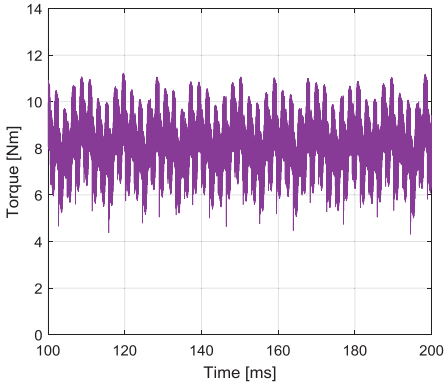

Fig. 14. Motor torque as a function of time for the unipolar method

Despite the pulsations in motor torque waveforms, the drive system speed remains practically constant. This is due to the high PWM frequency of inverter operation and the inertia of the motor rotor. Speed pulsations amount to 1% and 0.44% of the mean value for the bipolar method and the unipolar method, respectively.

Power losses in the rotor (Figs. 15–16) are caused by magnetic flux pulsations with the following frequencies: 15 625 Hz – PWM, 450 Hz – winding phases commutation, 100 Hz – voltage ripples at the inverter input and 900 Hz – the stator slotting. An FFT analysis of the

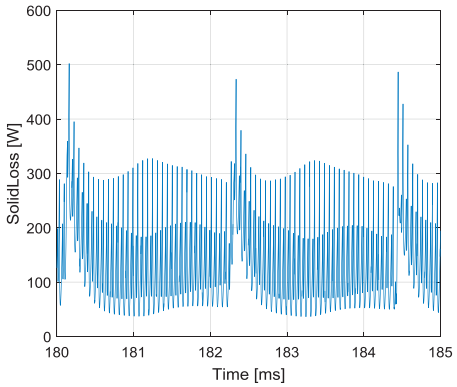

Fig. 15. Total power losses in the magnets and the rotor yoke as a function of time for the bipolar method

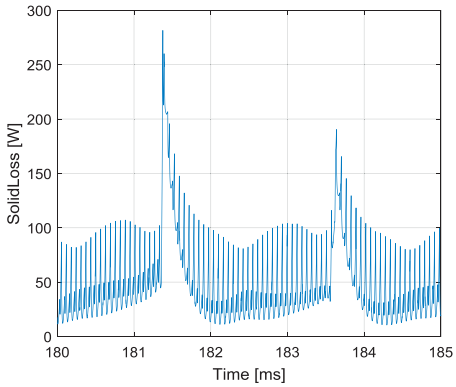

Fig. 16. Total power losses in the magnets and the rotor yoke as a function of time for the unipolar method

waveforms of power losses in the rotor showed that for both the bipolar method and the unipolar method, the losses are mainly caused by magnetic flux pulsations with the PWM frequency.

At the PWM frequency (15 625 Hz) the depth of magnetic flux density penetration into the rotor amounts to several millimetres and is only slightly greater than the height of the magnets (3.5 mm). For this reason, power losses in the rotor occur mainly in the permanent magnets, and so the rotor yoke does not need to be made of laminated sheet steel.

Similarly as in the case of rotor power losses, the losses resulting from inverter PWM operation constitute a considerable part of the stator core power losses (Figs. 17, 18).

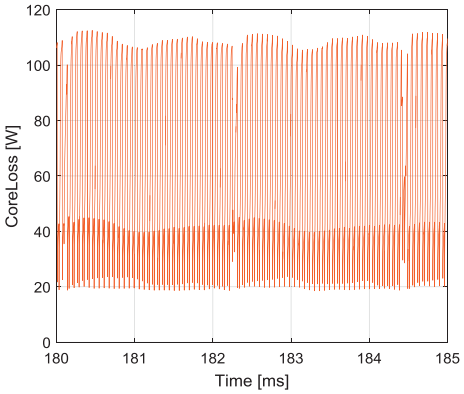

Fig. 17. Power losses in the stator core as a function of time for the bipolar method

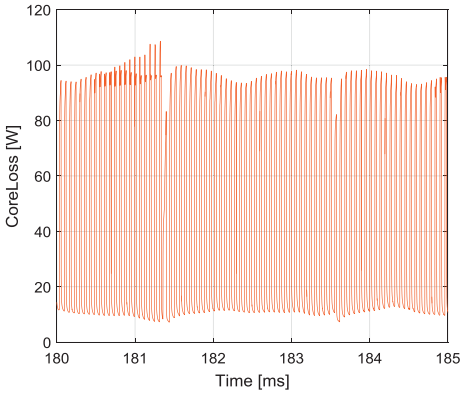

Fig. 18. Power losses in the stator core as a function of time for the unipolar method

Due to the higher amplitude of the phase current pulsations, the power losses in the stator core are about 63% higher for the bipolar method than for the unipolar method (Figs. 17, 18). Power losses in the rotor are also much higher (Figs. 15, 16). As a result of the higher motor losses, the motor efficiency for the bipolar method amounts to only 78.6%, whereas for the unipolar method it is as high as 87.1% (Table 1).

Table 1. Computed power losses and efficiencies of the drive system at different rotational speeds; $T = T_N = 8$ Nm

Parameter name	**Unit**	**Bipolar method**	**Unipolar method**
P	[W]	1 283	1 277
P_p	[W]	1 772	1 578
P_s	[W]	1 632	1 465
ΔP_p	[W]	140	113
ΔP_s	[W]	349	188
η_p	[%]	92.0	92.8
η_s	[%]	78.6	87.1
η	[%]	72.4	80.9

Where P is the motor mechanical power, P_p is the power consumed by the converter, P_s is the power consumed by the motor, ΔP_p are the converter power losses, ΔP_s are the BLDC motor power losses, η_p is the converter efficiency, η_s is the motor efficiency, η is the drive system efficiency.

5. Laboratory tests of the drive system

5.1. The test stand

The diagram of the measurement system is shown in Fig. 19, while the specially designed test stand can be seen in Fig. 20.

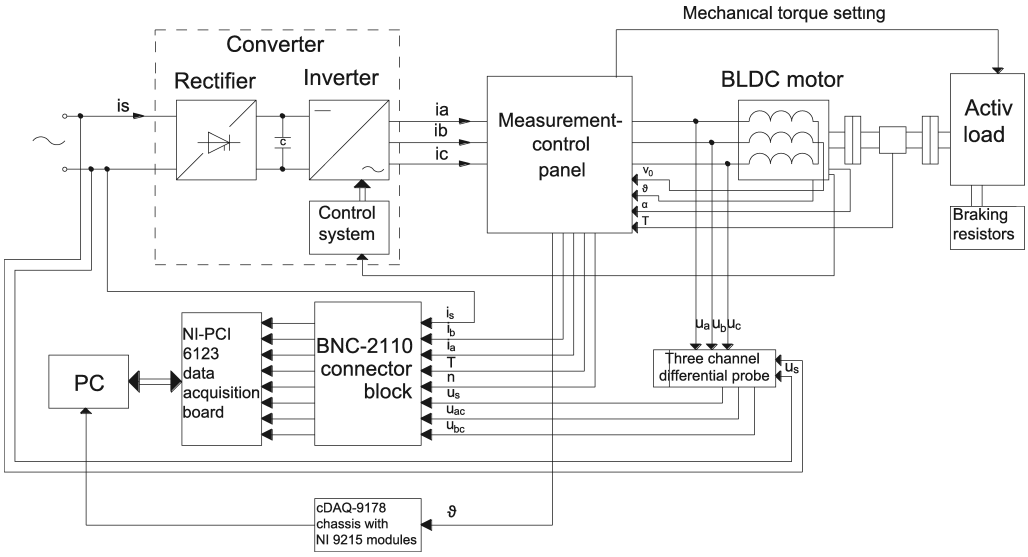

Fig. 19. Diagram of the measurement system: *is* is the instantaneous value of converter input current; *us* is the instantaneous value of converter input voltage; *ia*, *ib*, *ic* is the instantaneous values of motor phase currents; *ua*, *ub*, *uc* is the instantenous values of phase voltages; *uac*, *ubc* are the instantaneous values of motor line voltages; *v*0 is the winding star point potential; *n* is the rotational speed signal; *T* is the mechanical torque signal; α is the rotor position signal

The stand consists of: the tested motor with the power supply and control system, an active load (a servo motor, a servo drive controller and braking resistors), a torque transducer, a measuring and control panel with current transducers, a three-channel differential probe for voltage waveform measurement and a PC with data acquisition board and a LabVIEW program for recording and visualizing electrical and mechanical quantities. The stand enables the measurement of the waveforms of electrical and mechanical quantities in the single phase AC network-converter-BLDC motor system at different rotational speeds and different motor load torque values. The stand is described in detail in [15].

Fig. 20. View of the test stand

5.2. Analysis of the experimental results

Measurements of waveforms in the drive system were made at the rated load torque at different rotational speeds (from 500 to 3 000 rpm). The signal sampling frequency was 500 kHz. Exemplary results for the two speed control methods are shown in Figs. 21–24. Similarly as the field-circuit computation results presented in section 3, the exemplary results are for the rotational speed of 1 500 rpm and the inverter PWM operating frequency of 15 625 Hz.

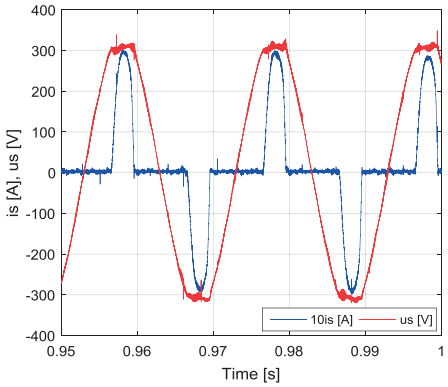

Fig. 21. Converter input current (*is*) and converter input voltage (*us*) as a function of time for the bipolar method

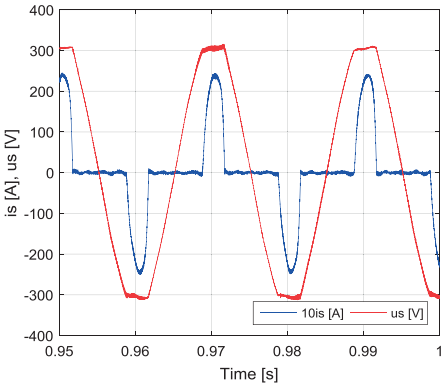

Fig. 22. Converter input current (*is*) and converter input voltage (*us*) as a function of time for the unipolar method

Using the measured waveforms, characteristics illustrating the dependence of the drive system power losses and efficiencies on rotational speed at the rated load torque were determined (Figs. 25–26).

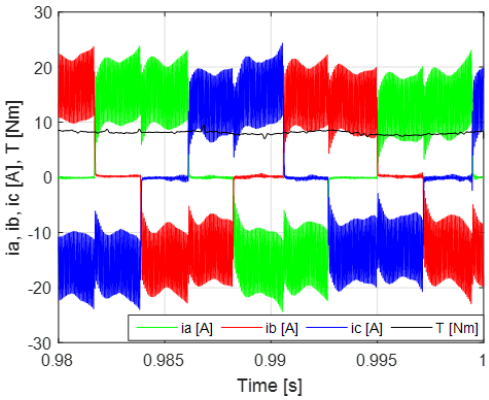

Fig. 23. Phase currents (*ia*, *ib*, *ic*) and mechanical torque (*T*) as a function of time for the bipolar method

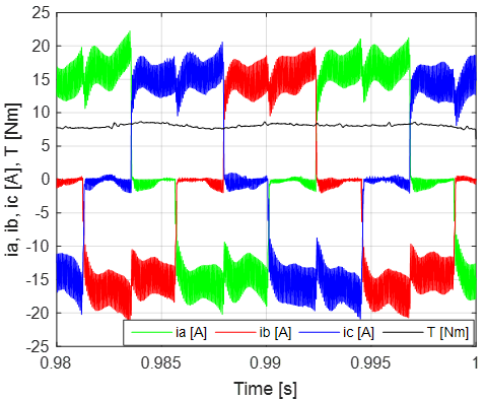

Fig. 24. Phase currents (*ia*, *ib*, *ic*) and mechanical torque (*T*) as a function of time for the unipolar method

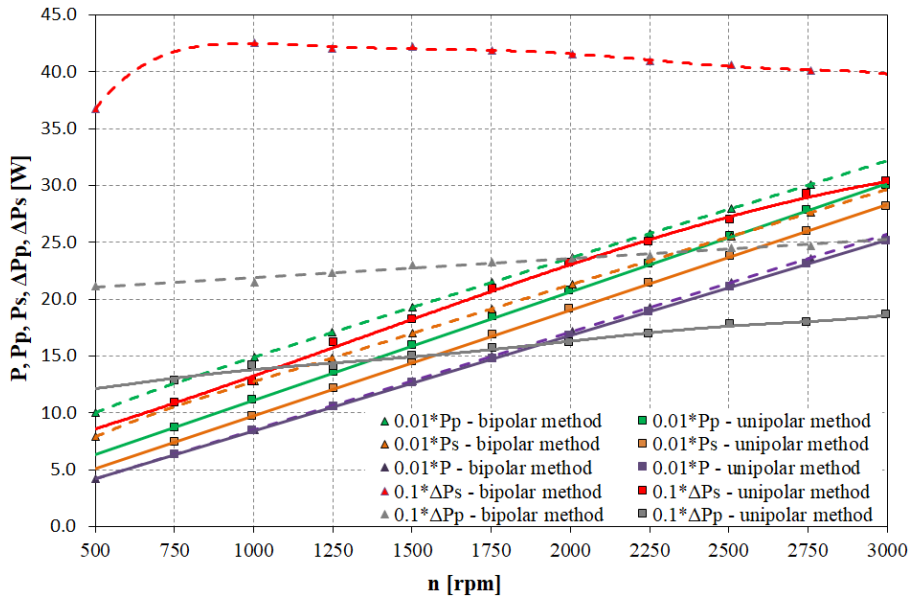

Fig. 25. Comparison, for the two control methods, of the dependence between the parameters of the drive system with the BLDC motor and rotational speed at constant load torque $T = T_N$

The results of the laboratory tests confirmed that the unipolar method is definitely a better method of controlling the rotational speed of BLDC motors than the bipolar method.

The measured waveforms are similar to the computed ones. A significant difference can be observed only in the case of the motor torque waveforms (Figs. 13, 14, 23, 24), which is due to the limitation of the torque transducer bandwidth.

In both the computation results and the measurement results, the steepness of the phase current decrease for the bipolar method is much higher than for the unipolar method. Consequently, as in the computation results (Figs. 11, 12), the pulsations of the motor phase currents resulting from inverter PWM operation are about twice higher for the bipolar method (Figs. 23, 24).

The measurements performed at different rotational speeds showed that the maximum values of phase currents are 3–17% higher for the bipolar method than for the unipolar method. Also the pulsations resulting from inverter PWM operation are 46.3–481% higher. As a result of the higher pulsations of phase currents, the losses in both the motor (from 31.6 to 421%) and the converter (from 36.0 to 73.7%) are much higher (Fig. 25, Table 2) for the bipolar method.

Consequently, both the motor efficiency and the converter efficiency are higher in the case of the unipolar method (Fig. 26, Table 2). The greatest differences in efficiency occur at low rotational speeds, which is due to the change in power loss values in the motor rotor.

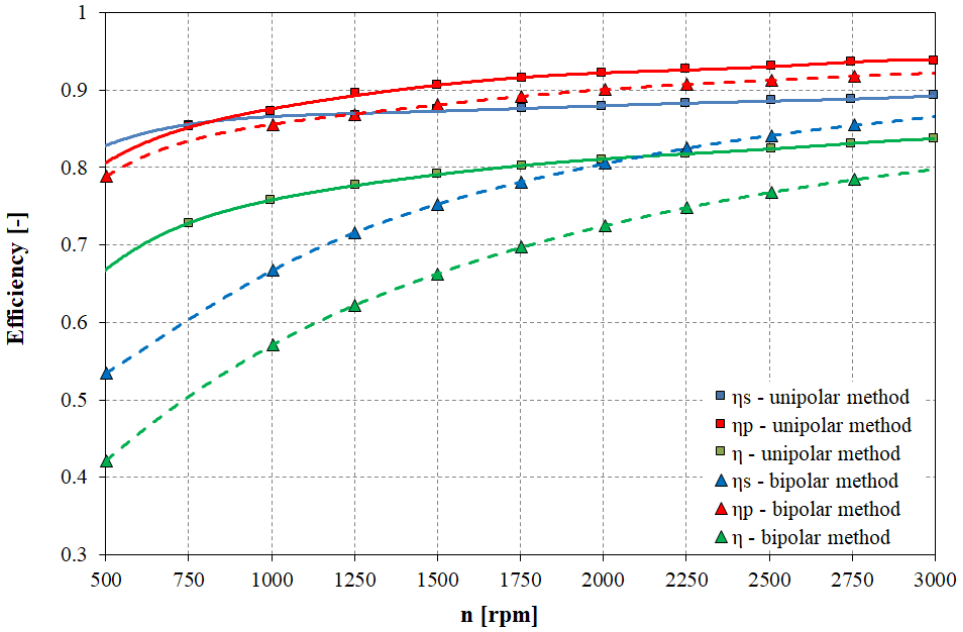

Fig. 26. Comparison of motor efficiency η_s, converter efficiency η_p and total system efficiency η for the two control methods; $T = T_N$

The motor efficiency measured at the nominal torque and the rotational speed of 1 500 rpm amounts to 75.2% for the bipolar method and to 87.4% for the unipolar method (Fig. 26, Table 2). In the case of the converter, the measured efficiency amounts to 88.0% and 90.6% for respectively the bipolar method and the unipolar method.

As a result of the higher power losses in the drive system, the average value of the converter input current for the bipolar method is from 6.7% to 47% higher. The maximum value of the converter input current is also higher (by approx. from 9% to 14%).

Table 2. Measured power losses and efficiencies of the drive system at different rotational speeds; $T = T_N = 8$ Nm

Parameter name	Unit	500 rpm		1 500 rpm		3 000 rpm	
		Bipolar method	Unipolar method	Bipolar method	Unipolar method	Bipolar method	Unipolar method
P	[W]	423	419	1 279	1 264	2 572	2 513
P_p	[W]	1 002	628	1 930	1 596	3 224	3 002
P_s	[W]	790	506	1 700	1 446	2 971	2 816
ΔP_p	[W]	212	122	230	150	253	186
ΔP_s	[W]	367	87	421	182	399	303
η_p	[%]	78.8	80.5	88.0	90.6	92.1	93.8
η_s	[%]	53.5	82.8	75.2	87.4	86.5	89.2
η	[%]	42.2	66.7	66.2	79.1	79.7	83.7

6. Conclusions

Field-circuit models of the BLDC motor with speed control for two PWM methods (the unipolar H_ON_L_PWM and the bipolar H_PWM_L_PWM) were developed. Using the models, waveforms of the electrical and mechanical quantities in the single-phase AC network-converter-BLDC motor system were determined. The results of the computations were verified by measurements performed on a specially designed test stand. The dependence of the drive system power losses and efficiencies on rotational speed was determined. Thanks to the computations and the measurements, the waveforms and operation of the drive system with the BLDC motor could be compared for the analysed speed control methods.

Considering the higher (by 4.0–24.5%) efficiency of the system (Table 2), the lower (by 6.3–31.9%) average value of the current drawn from the network and the lower (by 3.0–14.5%) maximum phase current values, the unipolar method of inverter control is definitely more advantageous.

Acknowledgements

The computations were performed using the resources of the Wroclaw Centre for Networking and Supercomputing (http://wcss.pl). Grant No. 400.

References

[1] Gieras J.F., Wing M., *Permanent magnet motor technology*, Marcel Dekker, Inc. New York, Basel (2002).

[2] Hendershot J.R., Miller T.J.E., *Design of brushless permanent-magnet motors*, Magna Physics Publishing and Calderon Press, Oxford (1994).

[3] Cui Ch., Liu G., Wang K., *A Novel Drive Method for High-Speed Brushless DC Motor Operating in a Wide Range*, IEEE Transactions on Power Electronics, vol. 30, iss. 9, pp. 4998–5008 (2015).

[4] Li Q., Huang H., Yin B., *The study of PWM methods in permanent magnet brushless DC motor speed control system*, International Conference on Electrical Machines and Systems, Wuhan, China 2008, pp. 3897–3900 (2008).

[5] Mijavec D., Zidari B., *Eddy current losses in permanent magnets of the BLDC machine*, COMPEL – the International Journal for Computation and Mathematics in Electrical and Electronic Engineering, vol. 26, iss. 4, pp. 1095–1104 (2007).

[6] Ishak D., Zhu Z.Q., Howe D., *Eddy-current loss in the rotor magnets of permanent-magnet brushless machines having a fractional of slots per pole*, IEEE Transactions on Magnetics, vol. 41, no. 9, pp. 2462–2469 (2005).

[7] Zhu Z.Q., Ng K., Schofield N., Howe D., *Improved analytical modelling of rotor eddy current loss in brushless machines equipped with surface-mounted permanent magnets*, IEE Proceedings – Electric Power Applications, vol. 15, no. 5, pp. 641–650 (2004).

[8] Deng F., *Commutation-caused eddy-current losses in permanent magnet brushless dc motors*, IEEE Transactions on Magnetics, vol. 33, pp. 4310–4318 (1997).

[9] Atallah K., Howe D., Mellor P.H., Stone D.A., *Rotor loss in permanent-magnet brushless AC machines*, IEEE Transactions on Industry Applications, vol. 36, iss. 6, pp. 1612–1618 (2000).

[10] Popescu M., Ionel D.M., Boglietti A., Cavagnino A., Cossar C., McGilp M.I., *A General Model for Estimating the Laminated Steel Losses Under PWM Voltage Supply*, IEEE Transactions on Industry Applications, vol. 46, iss. 4, pp. 1389–1396 (2010).

[11] Huang Y., Dong J., Zhu J., Guo Y., *Core Loss Modeling for Permanent-Magnet Motor Based on Flux Variation Locus and Finite-Element Method*, IEEE Transactions on Magnetics, vol. 48, no. 2, pp. 1023–1026 (2012).

[12] Kim K.C., *Analysis on Core Loss of Brushless DC Motor Considering Pulse Width Modulation of Inverter*, Journal of Electrical Engineering and Technology, vol. 9, no. 6, pp. 1914–1920 (2014).

[13] Ciurys M.P., *Time-stepping finite element analysis of a brushless DC motor with the PWM speed control*, IEEE Conference Publications, International Symposium on Electrical Machines (SME), Naleczow, Poland (2017).

[14] Ciurys M.P., Dudzikowski I., *Analysis of a brushless dc motor integrated with a high-pressure vane pump*, Technical Transactions Electrical Engineering, 1-E/2015, pp. 407-416 (2015).

[15] Ciurys M.P., Dudzikowski I., Pawlak M., *Laboratory tests of a PM-BLDC motor drive*, IEEE Conference Publications, Selected Problems of Electrical Engineering and Electronics (WZEE), Kielce, Poland (2015).

[16] Ciurys M.P., *Electromagnetic phenomena analysis in brushless DC motor with speed control using PWM method*, Open Physics, vol. 15, iss. 1, pp. 907–912 (2017).